Journal of Materials Chemistry C

Accepted Manuscript

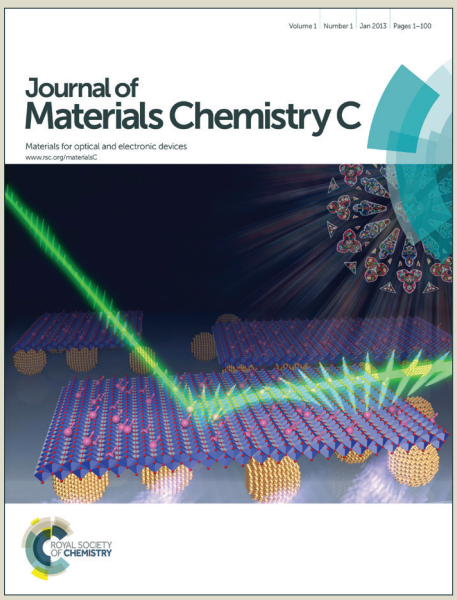

ROYAL SOCIETY OF CHEMISTRY

www.rsc.org/materialsC

Journal Name

RSCPublishing

ARTICLE

Direct White Light Emission from a Rare-Earth-Free Aluminium-Boron-Carbon-Oxynitride Phosphor

Cite this: DOI: 10.1039/x0xx00000x

T. Ogi*[,a], H. Iwasaki[b], A. B. D. Nandiyanto[a], F. Iskandar[c], W.-N. Wang[d], and K. Okuyama[e]

Received ooth January 2012,
Accepted ooth January 2012

DOI: 10.1039/x0xx00000x

www.rsc.org/

White light-emitting diodes offer the possibility of efficient, safe, and reliable solid-state lighting, and thus have various applications. Reported white light-emitting phosphors usually contain expensive rare-earth metals and are generally prepared by high-energy processes (e.g., >1000 °C, H_2 and CO reduction atmospheres). These factors limit their applications. Therefore, preparing cost-effective white light-emitting phosphors from environmentally friendly processes is an important challenge. Herein, a direct white light-emitting aluminium-boron-carbon-oxynitride (AlBCNO) phosphor, which can be economically produced using low-energy methods (<900 °C, atmospheric conditions), is reported. To the best of our knowledge, this is the first reported rare-earth-free white light-emitting phosphor. AlBCNO emission spans the entire visible spectrum, and its broad excitation spectrum is comparable to that of near-UV light-emitting diodes. Increasing the relative concentrations of B or Al in AlBCNO enables emission tuning to yellow or blue, respectively. These findings have implications for new methods of preparing white light-emitting phosphors.

Introduction

Solid-state lighting using white light-emitting diodes (LEDs) has attracted much attention because of its energy efficiency, safety, reliability, ease of maintenance, and environmental friendliness.[1-3] Two main methods are currently used to achieve white light emission from a LED chip. One method is to mix red-, green- and blue-LEDs. However, this approach is rarely used. It is costly and each LED chip has different drive voltages, thermal properties and degradation trends, which restricts its application. The other method is to use a blue- or UV-LED chip combined with down-converting the phosphors.[4-6] The most common way to create a white-LED is to combine a blue InGaN chip with a $Y_3Al_5O_{12}:Ce^{3+}$ (YAG:Ce)-based yellow phosphor.[7, 8] Devices based on this phosphor tend to exhibit a poor colour-rendering index and a high correlated colour temperature because of limited emitted red wavelengths, and this limits the LED's applications.[1] The blue component in white LEDs also reportedly causes retinal stress.[9]

Lighting systems that employ UV-LED chips using red, green, and blue phosphors (tricolour phosphors)[2] can potentially avoid these problems. This approach provides white LEDs with excellent colour-rendering indices, and these generate warm white light without blue component hazards. However, the luminescence efficiency of these systems is low because of the strong reabsorption of blue wavelengths by the red and green phosphors. It is also difficult to control the colour balance in tricolour systems, resulting in complicated and costly devices.

Single component white-emitting phosphors are non-blending red, green, and blue phosphors, and they are currently being investigated to overcome these problems. Much effort has been put into developing single component white-emitting phosphors, as detailed in Table SI-1.[1, 10-23] However, three distinct problems must be addressed before the currently available white LEDs can be commercially viable. First, expensive raw materials including rare-earth (RE) metals tend to be required for white light emission. Demand for these is likely to exceed supply and, therefore, it is important that newly developed materials are not dependent on RE metals. Second, most synthetic procedures require temperatures in excess of 1000 °C over extended periods. Reductive atmospheres are also often employed and require hydrogen and carbon monoxide to activate the RE ions, resulting in potential safety issues. Third, quantum yield is an important consideration for practical LED applications; however, few studies have reported the quantum yield of white light-emitting phosphors. In summary, an RE-free white light-emitting phosphor is highly desirable for next-generation solid-state lighting applications.

Boron carbon oxynitride (BCNO) phosphors[24] are good candidates for RE-free white light-emitting phosphors. Their advantages are (1) their composition of inexpensive B, C, N, and O, (2) their relatively low preparation temperatures (<900 °C) at ambient pressure, (3) their colour emission is tuneable from violet to near-red wavelengths (387–571 nm) by varying the C content, (4) their relatively high internal quantum efficiency (IQE), (5) their broad excitation spectrum (254–460 nm), and (6) the variety of morphologies obtainable including nanocrystals and fibers.[24-30] However, direct white emission from BCNO systems has not yet been reported. The emission colour in BCNO systems is determined by their C content. On the other hand, an alternative RE-free phosphor is $Al_2O_3:C$,[31] which has been developed using the same method as that used for BCNO. The $Al_2O_3:C$ phosphor exhibits intense blue emission under UV excitation. This unique property

suggests that if Al is introduced to the yellow-emitting BCNO phosphor, it will provide a broad range of luminescence, which will cover both the blue and yellow emission bands. Thus, the hybridization of yellow-emitting BCNO and blue-emitting Al_2O_3:C phosphors may allow the development of new white light-emitting phosphors. However, no previous study has been carried out to determine if RE-free white light-emitting materials can be used as novel phosphors.

Here, we report the facile synthesis of a RE-free white light-emitting phosphor containing Al, B, C, N, and O (AlBCNO). AlBCNO was prepared from RE-free raw materials, i.e. boric acid, urea, PEI, and aluminium hydroxide in a low-energy process (<900 °C, atmospheric conditions). Upon excitation at 365 nm, AlBCNO exhibited a broad emission band centred at 462 nm and spanning the entire visible spectrum. This resulted in excellent white light emission. Detailed characterization suggests that the AlBCNO phosphor is mainly composed of BCNO and Al_2O_3:C; but the phosphor is not just a simple mixture since the photoluminescence (PL) spectrum of AlBCNO is very different from that of physically mixed BCNO and Al_2O_3:C. To the best of our knowledge, this is the first reported RE-free white light-emitting phosphor. Furthermore, varying the relative concentrations of B and Al allows blue and yellow light generation with high colour stability.

Results and discussion

Figure 1(a) and (b) show the PL and photoluminescence excitation (PLE) spectra, respectively, for powder samples 1-3 prepared under the conditions shown in Table 1. Samples 1 and 2 were prepared as a representative model of the BCNO and Al_2O_3:C phosphors, respectively. The B/Al molar ratio of sample 3 was 2.00. Precursor solutions for all three samples were heated at 800 °C for 30 min under ambient pressure. For sample 3 (representative AlBCNO), a broad emission band centred at 462 nm was observed under excitation at 365 nm. This broad bands overlaps those of sample 2 (Al_2O_3:C) and sample 1 (BCNO), as they are centred at 450 and 500 nm, respectively. The full width at half maximum (FWHM) of the emission peak of AlBCNO is around 170 nm, which is larger than that of Al_2O_3:C and BCNO. This indicates that AlBCNO exhibits good colour rendering. The PLE spectrum of AlBCNO (Figure 1(b)), which was monitored at 462 nm, gave components at 358 (strongest) and 432 nm. The PLE spectra for Al_2O_3:C and BCNO, which were monitored at 450 and 500 nm, respectively, exhibited broad bands from 250 to 460 nm. The strongest AlBCNO peak at 358 nm is attributed to Al_2O_3:C at 349 nm and BCNO at 380 nm. The AlBCNO peak at 432 nm originates from Al_2O_3:C at 413 nm and BCNO at 468 nm. The PLE spectrum of AlBCNO is relatively broad with one high wavelength and several low wavelength peaks. AlBCNO can potentially be used as a direct white light-emitting source under UV- or visible-light excitation. Figure 1(c) and (d) show chromaticity analyses and digital photographs, respectively, of the three phosphor samples. The chromaticity coordinates (x, y) of AlBCNO, BCNO, and Al_2O_3:C were (0.28, 0.35), (0.30, 0.43), and (0.20, 0.14), respectively. Those of AlBCNO were the closest to typical values for white light emission (0.35, 0.35). Figure 1(d) shows digital photographs of the samples upon excitation at 365 nm. Figure 1(d1) shows that AlBCNO exhibits white light emission. Yellow emission and blue emission were observable by the naked eye for BCNO and Al_2O_3:C, respectively (Figure 1(d2) and (d3)). The internal quantum efficiency (IQE) values of AlBCNO, BCNO and Al_2O_3:C were 14.1, 25.1, and 9.4%, respectively. The IQE of AlBCNO is lower than that of previously reported white light-emitting phosphors (13–30%) composed of $Ca_4Y_6(SiO_4)_6O$:Ce^{3+}/Mn^{2+},Tb^{3+}.[17] However, AlBCNO has more potential because its synthesis does not require RE materials or high-energy processes. The environmentally friendly preparation of AlBCNO can potentially result in significant energy reduction.

Table 1 Precursor and synthesis temperature conditions of the produced phosphor samples.

Sample name	Boric Acid [mol/L]	Urea [molL]	PEI [mol/L]	$Al(OH)_3$ [mol/L]	B/Al [-]	Synthesis temperature
Sample 1	25.00	329.00	33.33	0.00		800°C
Sample 2	0.00	493.50	50.00	1.50	-	800°C
Sample 3	37.50	500.00	75.00	0.38	2.00	800°C
Sample 4	37.50	0.00	75.00	0.23	3.33	900°C
Sample 5	37.50	0.00	75.00	0.19	4.00	900°C
Sample 6	37.50	0.00	75.00	0.13	6.00	900°C
Sample 7	37.50	0.00	75.00	0.08	10.0	900°C
Sample 8	37.50	0.00	75.00	0.05	14.0	900°C
Sample 9	37.50	0.00	75.00	0.04	18.1	900°C

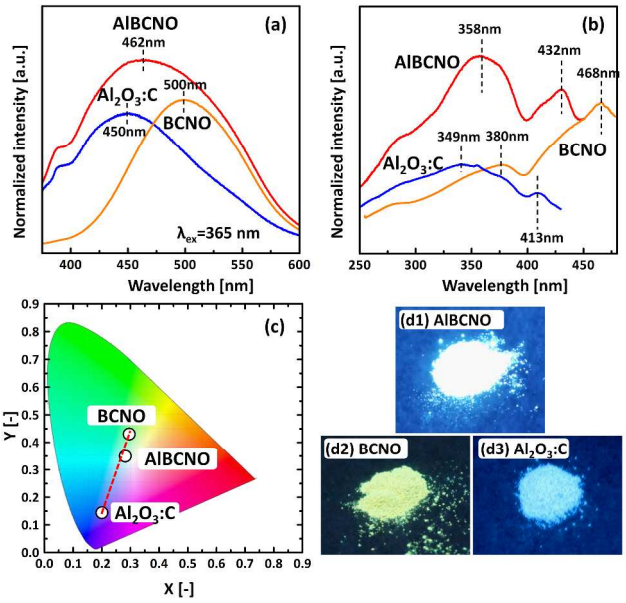

Figure 1 (a) Emission spectrum, (b) excitation spectrum, (c) colour diagram, and (d) digital photographs of the AlBCNO, Al_2O_3:C, and BCNO powder samples.

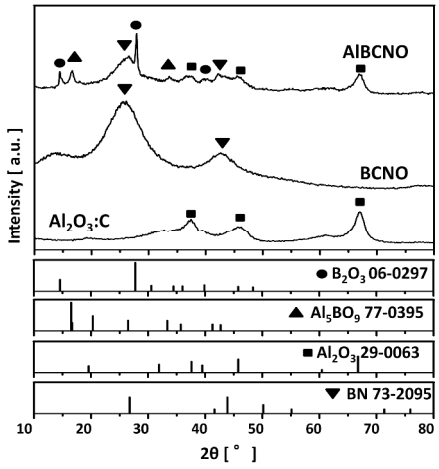

Figure 2 XRD patterns of the AlBCNO, BCNO, and Al_2O_3:C phosphors.

To investigate the white light emission from AlBCNO, the crystal structures and chemical compositions of several samples were analysed by X-ray diffraction (XRD), field emission scanning electron microscopy (FESEM) and high-resolution transmission electron microscopy (HRTEM). The XRD pattern (Figure 2) of Al_2O_3:C corresponded well to that of Al_2O_3 [JCPDS 29-0063], and that of BCNO corresponded to that of BN [JCPDS 73-2095]. These results are in agreement with previous reports.[24,31] XRD peaks corresponding to B_2O_3 [JCPDS 06-0297], Al_5BO_9 [JCPDS 77-0395], Al_2O_3, and BN were also observed in the spectrum of the AlBCNO sample. Thus, AlBCNO contained crystalline BCNO and Al_2O_3:C, and new B_2O_3 and Al_5BO_9 crystal phases were also formed. These results are supported by the FESEM observations shown in Figure 3(a–d). Figure 3(c, d) shows that sample 1 (BCNO) is composed of flake-shaped particles larger than 3 μm, and sample 2 (Al_2O_3:C) is composed of near-spherical particles smaller than 300 nm. The morphology of AlBCNO is shown in Figure 3(a) and (b), and the flake-shaped particles are composed of needle-like crystals. AlBCNO particles should be expected to appear as mixed Al_2O_3:C and BCNO materials in which Al_2O_3:C is coated by BCNO. Needle-like crystals have been previously observed for Al_5BO_9.[32]

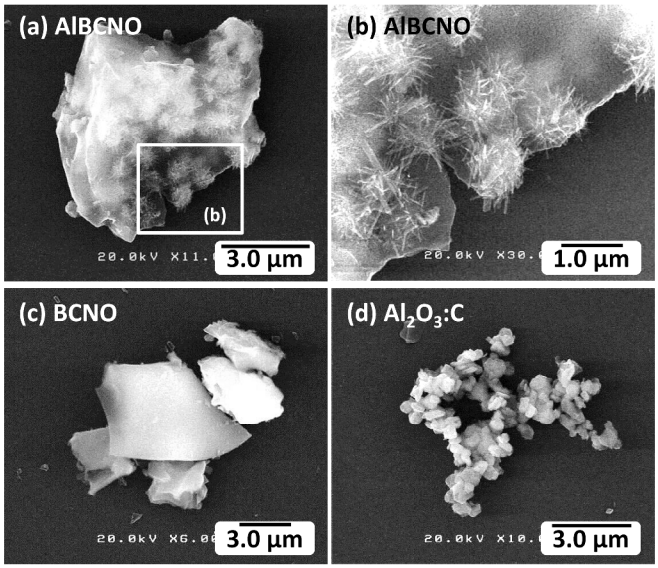

Figure 3 SEM images of the AlBCNO, BCNO, and Al_2O_3:C phosphor samples.

The AlBCNO particle morphology and the local structure of the elemental states were analysed using TEM and electron energy loss spectroscopy (EELS). Figure 4(a1) and (a2) show TEM images of AlBCNO. Some particles larger than 300 nm (Figure 4(a1)) were surrounded by amorphous material. The TEM image (Figure 4(a2)) shows that needle-like crystals also exist within the flake-shaped particle. HRTEM images were obtained from the positions indicated in Figure 4(a1) and (a2) and are shown in Figure 4(b1–3). Figure 4(b1) shows that the flake-shaped particles consist of amorphous material and nanocrystals smaller than 5 nm. Most nanocrystals had a lattice spacing of 0.32 nm, and this is consistent with the (002) plane of BN (JCPDS 73-2095). Previous reports[24] suggest this position indicates turbostratic boron nitride (t-BN). The HRTEM observation at position 2 in Figure 4(a1) showed microcrystals with a lattice spacing of 0.24 nm. This may be due to the (311) plane of Al_2O_3 (JCPDS 29-0063). High crystallinity was observed for the needle-shaped samples shown in Figure 4(b3). These nanocrystals had a lattice spacing of 0.53 nm, indicating the (020) plane of Al_5BO_9 (JCPDS 77-0395).

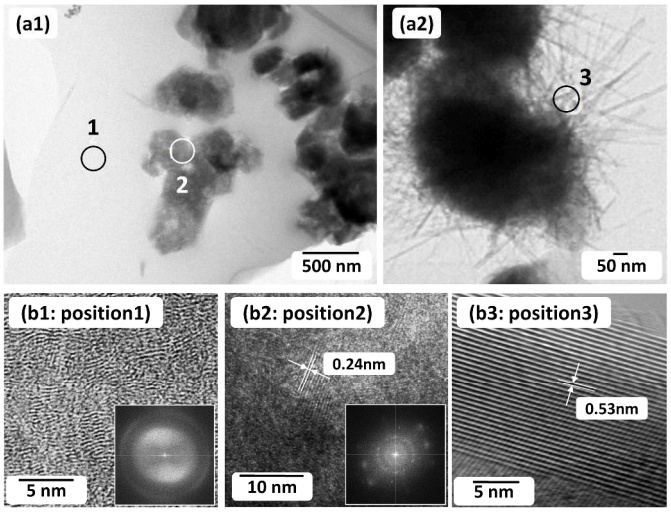

Figure 4 TEM analysis of the AlBCNO phosphor sample; (a) TEM images and (b) HRTEM images.

Figure 5 shows the EELS spectra obtained at positions 1 (film) and 2 (particle), as indicated in Figure 4(a1). The results show that B, C, N and O are present in the film (position 1), and Al and O are mainly present in the crystallized particle (position 2). The result obtained for the film is similar to previous EELS results for BCNO.[24] The sharp B–K ionization peak at 194 eV (Figure 5(c)) and the three C–K ionization peaks at 285, 288, and 295 eV (Figure 5(d)) indicate that B is predominantly surrounded by N and O. This implies that there is little B–C bonding.[33] It also suggests a soft sp^2 hybridized C framework[34] within the film. A 7 eV peak was detected in the low loss spectrum (Figure 5(a)), which indicated an interband transition for BN.[35] Thus, BN bonding containing strong σ* bands exists in the film. Al–L ionization at 78.9 eV (Figure 5(b)), N–K ionization at 401 eV (Figure 5(e)), and O–K ionization at 540 eV (Figure 5(f)) were observed in the particle. Wu et al.[36] attributed these peaks to Al-N and Al-O bands. Weak characteristic peaks of B, C, and N were observed in the spectrum of the particle; however, the particles were covered to some degree by the film.

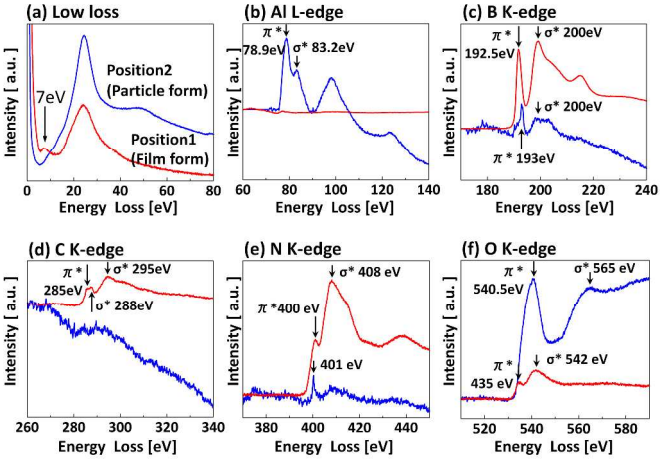

Figure 5 EELS analysis of the AlBCNO phosphor sample; red and blue spectra indicate the results from positions 1 and 2, as shown in Figure 4(a1).

Elemental mapping of Al, B, C, N, and O was undertaken for confirmation (Figure 6). These results indicated that the particles were composed of Al, B, C, N, and O. Al and O were predominantly located in the particles while B, C, N, and O were located in the film. X-ray fluorescence (XRF) analysis indicated an AlBCNO composition of 7.9, 9.73, 19.2, 13.5, and 49.7% for Al, B, C, N, and O, respectively. To summarize, the AlBCNO phosphor is a composite of flake-shaped particles and needle-like crystals. The flake-shaped particles are mainly composed of low-crystallinity t-BN including covalently bounded B, N, and O, with a sp^2 hybridized C framework, which is a representative BCNO. On the other hand, the needle-like crystals predominantly consist of highly crystalline Al_5BO_9 and microcrystalline Al_2O_3 contacting Al-N and Al-O bands and minor carbon impurities.

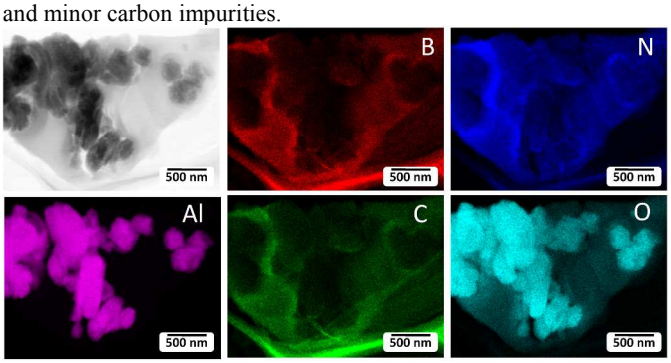

Figure 6 Elemental mapping of the AlBCNO phosphor sample.

The proposed particle formation mechanism is shown in Figure 7. The precursor solution of boric acid, urea, aluminium hydroxide and PEI was heated at 130 °C, and B_2O_3 was formed upon solvent evaporation (R1). At higher than 186 °C, B_2O_3 was gradually nitrided by the NH_3 generated from urea decomposition (R2). PEI then decomposed at higher than 300 °C,[29] and partially nitrided B_2O_3 (t-BN) containing C (BCNO) began to form at 450 °C (R3). At this temperature, the AlOOH crystals also formed from $Al(OH)_3$ (R4). At 480 °C, the B_2O_3 related materials began to melt and the AlOOH particles were surrounded by BCNO. At higher than 500 °C, Al_2O_3 and Al_5BO_9 crystals were generated (R5-R6). Minor carbon impurities likely exist within the Al_2O_3 crystals (namely, Al_2O_3:C). In summary, AlBCNO is composed of BCNO and Al_2O_3:C. When AlBCNO is excited at the appropriate wavelength, the BCNO emitted yellow wavelengths and the Al_2O_3:C emitted blue wavelengths. Overall, white light was emitted.

The PL properties of AlBCNO and physically mixed samples of Al_2O_3:C and BCNO were compared. Al_2O_3:C (sample 2) and BCNO (sample 1) powder samples were mixed at Al_2O_3:C:BCNO mass ratios of 1:1, 1:2, and 1:3, and the PL was measured at room temperature upon excitation at 365 nm (Figure SI-2). The FWHM of the spectrum for physically mixed 1:1 Al_2O_3:C:BCNO was 108 nm, and this was smaller than that of AlBCNO (170 nm). As a result, the emission of the mixed sample appeared green to the naked eye. This is attributed to the different PL intensities of each component. The PL intensity of BCNO was higher than that of Al_2O_3:C and, therefore, a red-shifted emission was observed in the mixed sample. Another reason for the colour heterogeneity could be inhomogeneous mixing since it is difficult to homogenously mix two powders. Mixing the materials during precursor preparation ensured that BCNO and Al_2O_3:C were well mixed at the atomic level in AlBCNO. However, AlBCNO is not a pure mixture of Al_2O_3:C and BCNO because crystalline Al_5BO_9 and B_2O_3 are also present.

Physically mixed powder samples were also heated at 800 °C for 30 min and their PL properties were measured at 365 nm. Figure SI-2(b) shows that heating mixed samples did not yield similar emission spectra to that of AlBCNO. This further supports the conclusion that AlBCNO is not a pure mixture of Al_2O_3:C and BCNO. The white-emission mechanism of AlBCNO is complicated and requires further investigation.

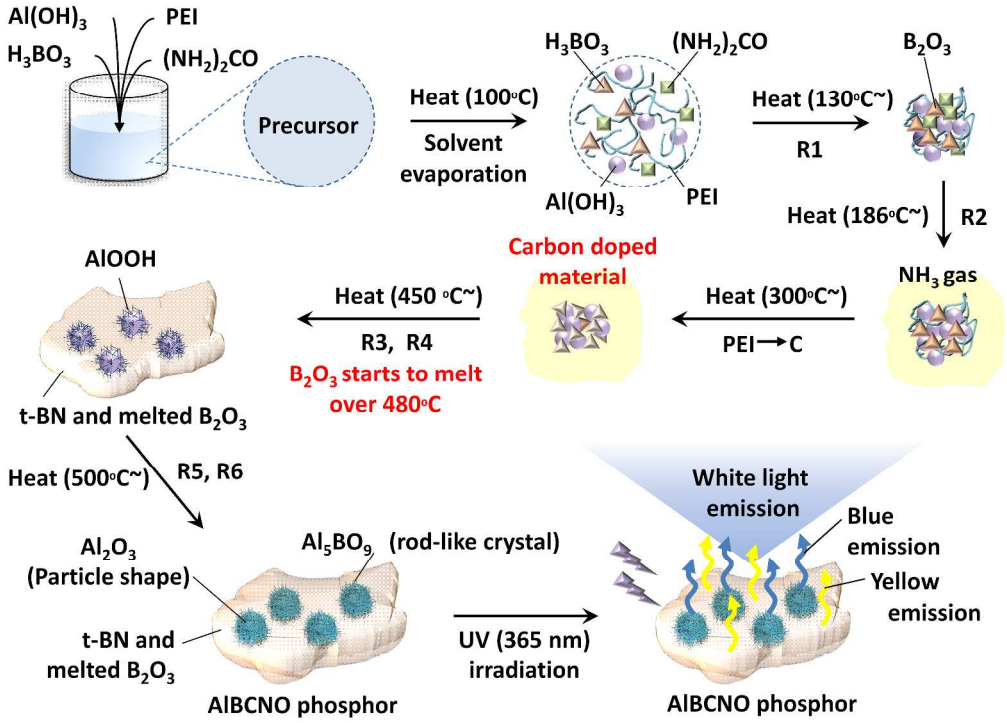

Figure 7 Particle formation and emission of AlBCNO phosphor;
R1; $2H_3BO_3 \rightarrow B_2O_3 + 3H_2O$ (130°C ~), R2; $(NH_2)_2CO \rightarrow C_2H_5N_3O_2 + NH_3$ (186°C ~), R3; $B_2O_3 + NH_3 \rightarrow 2BN$(t-BN) $+ 3H_2O$ (500°C ~), R4; $Al(OH)_3 \rightarrow 2AlOOH + H_2O$ (450°C ~), R5; $2AlOOH \rightarrow \gamma\text{-}Al_2O_3 + H_2O$ (500°C ~), R6; $\gamma\text{-}Al_2O_3 + 5B_2O_3 \rightarrow 2Al_5BO_9$ (800°C ~)

Urea was removed from the precursor solution to lower the production cost of AlBCNO. Previous reports suggest that PEI promotes nitridation.[29] PEI can potentially act as an N source for AlBCNO. Figure SI-3 compares the PL properties of AlBCNO with and without urea in the precursor solution. There is no significant difference in the spectrum, peak position, or chromaticity coordinates. According to our previous study,[29] thermal decomposition of PEI occurs from around 300 °C. Therefore, the nitrogen atoms derived from PEI at this temperature and the nitridation of the intermediate product were apparent without the use of urea.

PL and XRD measurements were obtained for AlBCNO prepared from precursor solutions with B/Al ratios of 3.33 to 18.1. In this experiment, the AlBCNO phosphors were prepared at 900 °C in expectation of an enhancement in quantum efficiency. Figure 8(a) shows the PL spectra of multi-colour emitting AlBCNO prepared using various B/Al ratios. An increase in ratio from 3.33 to 18.1 led to a red-shift in emission from 394 to 488 nm. The emission shifted to longer wavelengths with an increase in B content because the content of yellow-emitting BCNO also increased. This result is supported by XRD measurements (Figure SI-4), in which the BN peak intensity increases with an increase in the B/Al ratio. The red-shift of the maximum peak intensity is attributed to the increase in BCNO content. A low B/Al ratio results in the Al_2O_3:C and Al_5BO_9 phases dominating the powder sample and, therefore, the resulting phosphor exhibits blue emission. These phenomena are consistent with the AlBCNO emission mechanism proposed in Figure 7, and they show the importance of controlling the BCNO and Al_2O_3:C content of AlBCNO. The emission of AlBCNO can potentially be tuned from 394 to 488 nm. A chromaticity analysis was performed to further investigate the PL properties of the AlBCNO phosphors (Figure 8(b)). The chromaticity coordinates (x, y) of the AlBCNO phosphors with B/Al ratios of 3.33, 4.00, 6.00, 10.0, 14.0 and 18.1, were (0.177, 0.130), (0.184, 0.143), (0.211, 0.247), (0.237, 0.298), (0.288, 0.346), and (0.291, 0.354), respectively. The corresponding IQE values were 17.1, 19.0, 30.9, 35.4, 14.8, and 10.5%, respectively.

Although a more detailed study is required to determine the factors required for an increase in IQE and to better understand the emission mechanism, AlBCNO is a promising direct white light-emitting phosphor since it can be prepared without RE metals or high-energy processes. Such a preparation can lead to a significant energy reduction and can potentially be scaled-up for industrial application.

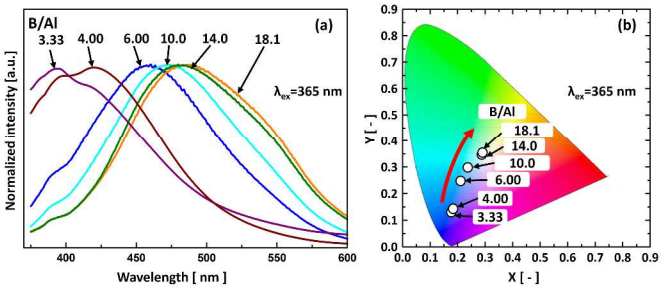

Figure 8 Effect of the B/Al ratios of the AlBCNO phosphor samples on the PL properties. Emission spectra (a), and colour diagram (b).

Conclusions

An RE-free white light-emitting AlBCNO phosphor was prepared from a precursor solution consisting of relatively inexpensive raw materials, i.e. boric acid, urea, PEI and aluminium hydroxide. The AlBCNO phosphor prepared at 800 °C exhibited a broad excitation band at 300–450 nm and a broad emission band centred at 462 nm. The chromaticity coordinate (x, y) and internal quantum efficiency of this AlBCNO phosphor were (0.28, 0.35) and 25.1%, respectively. XRD, TEM, and EELS analyses revealed that the AlBCNO was composed of low-crystallinity t-BN including covalently bound B, N and O, with a sp^2 hybridized C framework, highly crystalline Al_5BO_9, and microcrystalline Al_2O_3 contacting Al-N and Al-O bands and minor carbon impurities. Furthermore, the AlBCNO phosphor was not a simple mixture of the yellow emission from BCNO and the blue emission from Al_2O_3:C. In addition, the emission wavelength of AlBCNO can be tuned from 394 to 488 nm by changing the B/Al ratios from 3.33 to 18.1. The IQE value reached 35.4% when the B/Al ratio and the operating temperature were 10.0 and 900 °C, respectively. Even though the white-emission mechanism of AlBCNO requires further investigation, AlBCNO shows promise for white light-emitting applications because of its fascinating properties, low energy requirements and the low cost of preparation.

Experimental

Synthesis of phosphor samples. AlBCNO, BCNO, and Al_2O_3:C were prepared from liquid precursors. The synthetic method is shown in Figure SI-1. Phosphor precursors were prepared by dissolving boric acid (H_3BO_3, Wako Chemicals Co., Ltd., Japan), urea ($(NH_2)_2CO$, Wako Chemicals Co., Ltd.), polyethyleneimine (PEI) ($(-CH_2CHNH-)_n$, M_w=1800, Tokyo Chemical Industry Co., Ltd., Japan), and aluminium hydroxide ($Al(OH)_3$, Showa Denko K. K., Japan) in distilled water at 40 °C.

The concentrations of boric acid, urea, PEI and aluminium hydroxide used in the precursor solutions are shown in Table 1. The B/Al molar ratio of the precursor solutions varied from 2.00 to 18.1. The mixed precursors were transferred into a ceramic crucible and heated at 800–900 °C for 30 min under ambient pressure, and then cooled to room temperature.

Photoluminescence measurements. The PL and PLE spectra were measured at room temperature using a spectrofluorophotometer (RF-5300PC, Shimadzu Corp., Kyoto, Japan) equipped with an Xe lamp. The IQE and Commission Internationale de I'Eclairage (CIE) chromaticity coordinates for all the phosphors were measured using an absolute PL quantum yield measurement system (C9920-02, Hamamatsu Photonics, Shizuoka), with a $BaSO_4$-coated integrating sphere and a Xe lamp source. The PL analyses were performed at room temperature under excitation at 365 nm, which is a standard long UV excitation wavelength.

Materials characterization. Crystal structures were investigated using powder XRD (RINT 2200 V, Rigaku, Tokyo, Japan) with Cu Kα radiation. Morphologies and crystal sizes were observed by FESEM (S-5000, Hitachi Corp., Tokyo, Japan) at 20 kV, and HRTEM (JEM-3000F, JEOL, Tokyo, Japan) at 300 kV. The chemical compositions of the AlBCNO phosphors were investigated by EELS using a spectrometer attached to the HRTEM instrument. The spectral imaging of the powder samples was carried out using a JEOL JEM-3000F microscope (297 kV) equipped with a post column 90° energy filter (Gatan GIF-2000). Elemental mapping was obtained by the three windows technique from the spectral images. XRF analysis was used to determine the chemical compositions.

Table S1 Summery of single component white-emitting-phosphor.

Materials	method	operating condition	Emission	excitation	Quantum efficiency	Ref.
$Ba_3MgSi_3O_8:Eu^{2+},Mn^{2+}$	solid state reaction	unknown	442, 505, 620 nm	375 nm	unknown	6a)
$Sr_3MgSi_2O_8:Eu^{2+}$, $Sr_3MgSi_2O_8:Eu^{2+}$, Mn^{2+}	solid-state reaction	1250°C for 4 h under H_2 /N_2 atmosphere	470, 570, 680 nm	375 nm	unknown	6b)
Porous Zinc Gallophosphate	hydrothermal	160 °C for 7 days and heated at 280 °C for 4 h	433, 550 nm	390 nm	unknown	6c)
$Sr_3B_2O_6:Ce^{3+},Eu^{2+}$	solid state reaction	900–1000 °C under 15% H_2 /Ar atmosphere	434, 574 nm	351 nm	unknown	6d)
$Sr_3Al_2O_5Cl_2:Ce^{3+},Eu^{2+}$	solid-state reaction	1250 °C for 2 h under CO atmosphere	444, 609 nm	330 nm	unknown	6e)
$Ca_9Gd(PO_4)7:Eu^{2+},Mn^{2+}$	solid state reaction	1200°C for 4h under H_2 /N_2 atmosphere	490, 645 nm	254-430 nm	unknown	1
$Ca_3Y(GaO)_3(BO_3)_4:Ce^{3+},Mn^{2+},Tb^{3+}$	solid-state reaction	1000°C for 8 h under H_2 /N_2 atmosphere	409, 589 nm	365 nm	unknown	6f)
$Ca_4Y_6(SiO_4)_6O$: $Ce^{3+}/Mn^{2+}/Tb^{3+}$	solid state reaction	1350 °C for 2 h	410, 614 nm	284-424 nm	13-30%	7
$LiSr_4(BO_3)_3:Ce^{3+}$, Eu^{2+}	solid-state reaction	1227 °C for15h under H_2 /N_2 atmosphere	430, 612nm	350 nm	unknown	6g)
$Na(Sr,Ba)PO_4:Eu^{2+}$, Mn^{2+}	solid-state reaction	1150 °C for 10 h under H_2 /N_2 atmosphere	440-450, 600 nm	390 nm	unknown	6h)
Dy^{3+}-activated $Ba_3Bi(PO_4)_3$	solid-state reaction	1250 °C for 3 h	487, 575 nm	393 nm	unknown	6i)
$CaScAlSiO_6:Ce^{3+},Tb^{3+},Mn^{2+}$	solid state reaction	1400 °C for 4 h under H_2 /N_2 atmosphere	380, 542, 574, 670 nm	330 nm	unknown	6j)
$Ca_2YF_4PO_4:Eu^{2+},Mn^{2+}$	solid state reaction	1000 °C for 10 h in H_2/N_2	570 nm	375 nm	17.1-22%	6k)

Supporting Information

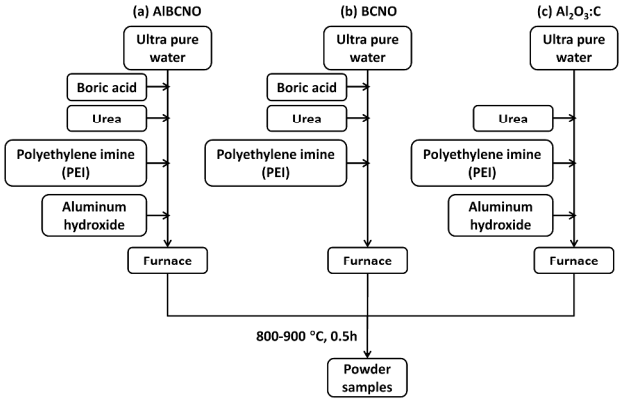

Figure SI-1 Experimental method.

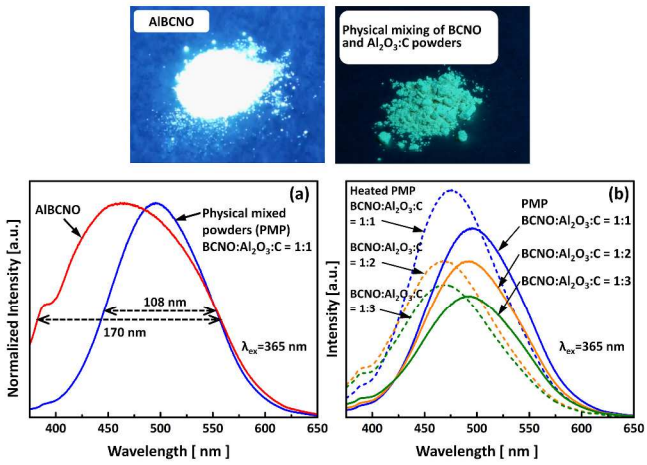

Figure SI-2 (a) Comparison of the photoluminescence properties between the AlBCNO phosphor and the physically mixed powder sample of the BCNO and Al_2O_3:C powders, (b) Effects of mixing ratios and heating (800 °C, 30 min) on the photoluminescence properties.

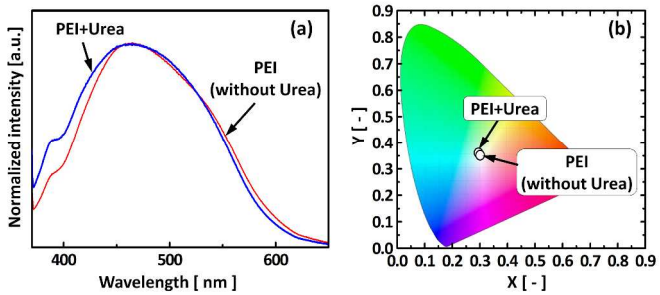

Figure SI-3 Effect of urea on the PL properties. Emission spectra (a) and colour diagram (b). Synthesis temperature: 800 °C.

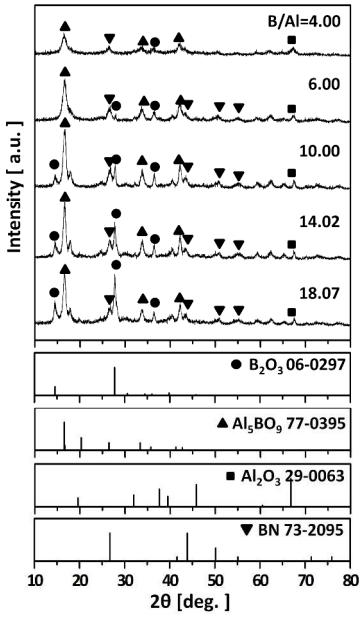

Figure SI-4 Effect of the B/Al ratio of the AlBCNO phosphor samples on the crystal structures.

Acknowledgements

This research was supported by JSPS KAKENHI (Nos. 30508809, 24656413) and JST No. AS242Z01588M. The authors thank Kousuke Okino for assistance with the experiments and with powder characterization, and Dr. Eishi Tanabe, Hiroshima Prefectural Institute of Industrial Science and Technology, for assistance with TEM and elemental mapping analyses.

Notes and references

[a] Department of Chemical Engineering, Graduate School of Engineering, Hiroshima University, 1-4-1 Kagamiyama, Higashi-Hiroshima 739-8527, Japan
[b] Battery Materials Laboratory, Kurashiki Research Center, Kuraray, Co., Ltd., 2045-1 Sakazu, Kurashiki, Okayama 710-0801, Japan
[c] Department of Physics, Institute of Technology Bandung, Ganesha 10, Bandung 40132, West Java, Indonesia
[d] Department of Energy, Environmental and Chemical Engineering, Washington University in St. Louis, 1 Brookings Drive, St. Louis, MO 63130, USA

1. Guo, N.; You, H.; Song, Y.; Yang, M.; Liu, K.; Zheng, Y.; Huang, Y.; Zhang, H. *J. Mater. Chem.* 2010, **20**, (41), 9061.

2. Lin, C. C.; Liu, R.-S. *J. Phys. Chem. Lett.* 2011, **2**, (11), 1268.

3. Liu, F.; Budai, J. D.; Li, X.; Tischler, J. Z.; Howe, J. Y.; Sun, C.; Meltzer, R. S.; Pan, Z. *Adv. Funct. Mater.* 2012.

4. Feldmann, C.; Jüstel, T.; Ronda, C. R.; Schmidt, P. J., *Adv. Funct. Mater.* 2003, **13**, (7), 511.

5. Li, Y.; Hirosaki, N.; Xie, R.; Takeda, T.; Mitomo, M., *Chem. Mat.* 2008, **20**, (21), 6704.

6. Yang, W.-J.; Luo, L.; Chen, T.-M.; Wang, N.-S., *Chem. Mat.* 2005, **17**, (15), 3883.

7. Birkel, A.; Denault, K. A.; George, N. C.; Doll, C. E.; Héry, B.; Mikhailovsky, A. A.; Birkel, C. S.; Hong, B.-C.; Seshadri, R., *Chem. Mat.* 2012, **24**, (6), 1198.

8. Nakamura, S.; Pearton, S.; Fasol, G., The blue laser diode: the complete story. *Springer*: 2000.

9. Peng, M.-L.; Tsai, C.-Y.; Chien, C.-L.; Hsiao, J. C.-J.; Huang, S.-Y.; Lee, C.-J.; Lin, H.-Y.; Wen, Y.-C.; Tseng, K.-W., Life Science Journal 2012, **9**, (1).

10. Kim, J. S.; Jeon, P.; Choi, J.; Park, H.; Mho, S.; Kim, G., *Appl. Phys. Lett.* 2004, **84**, 2931.

11. Kim, J. S.; Jeon, P. E.; Park, Y. H.; Choi, J. C.; Park, H. L.; Kim, G. C.; Kim, T. W., *Appl. Phys. Lett.* 2004, **85**, (17), 3696.

12. Liu, Y.; Lei, B.; Shi, C., *Chem. Mat.* 2005, **17**, (8), 2108.

13. Wang, M.-S.; Guo, S.-P.; Li, Y.; Cai, L.-Z.; Zou, J.-P.; Xu, G.; Zhou, W.-W.; Zheng, F.-K.; Guo, G.-C., J. Am. Chem. Soc. 2009, **131**, (38), 13572.

14. Chang, C.-K.; Chen, T.-M., *Appl. Phys. Lett.* 2007, **91**, 081902.

15. Song, Y.; Jia, G.; Yang, M.; Huang, Y.; You, H.; Zhang, H., S *Appl. Phys. Lett.* 2009, **94**, 091902.

16. Huang, C.-H.; Chen, T.-M., *J. Phys. Chem. C* 2011, **115**, (5), 2349.

17. Li, G.; Zhang, Y.; Geng, D.; Shang, M.; Peng, C.; Cheng, Z.; Lin, J., *ACS Appl. Mater. Interfaces* 2011, **4**, (1), 296.

18. Wang, Q.; Deng, D.; Hua, Y.; Huang, L.; Wang, H.; Zhao, S.; Jia, G.; Li, C.; Xu, S., *J. Lumines.* 2012, **132**, (2), 434.

19. Choi, S.; Yun, Y. J.; Jung, H.-K., *Mat. Lett.* 2012, **75**, 186.

20. Liu, Q.; Liu, Y.; Yang, Z.; Han, Y.; Li, X.; Fu, G., *J. Alloy. Compd.* 2012, **515**, 16.

21. Fang, X.; Roushan, M.; Zhang, R.; Peng, J.; Zeng, H.; Li, J., *Chem. Mat.* 2012, **24**, (10), 1710.

22. Lu□, W.; Guo, N.; Jia, Y.; Zhao, Q.; Lv, W.; Jiao, M.; Shao, B.; You, H., *Inorg. Chem.* 2013, **52**, (6), 3007.

23. Geng, D.; Shang, M.; Zhang, Y.; Cheng, Z.; Lin, J., *Eur. J. Inorg. Chem.* 2013, **2013**, (16), 2947.

24. Ogi, T.; Kaihatsu, Y.; Iskandar, F.; Wang, W. N.; Okuyama, K., *Adv. Mat.* 2008, **20**, (17), 3235.

25. Wang, W. N.; Kaihatsu, Y.; Iskandar, F.; Okuyama, K., *Mater. Res. Bull.* 2009, **44**, (11), 2099.

26. Kaihatsu, Y.; Wang, W. N.; Iskandar, F.; Ogi, T.; Okuyama, K., *J. Electrochem. Soc.* 2010, **157**, (10), J329.

27. Suryamas, A. B.; Munir, M. M.; Ogi, T.; Khairurrijal; Okuyama, K., *J. Mater. Chem.* 2011, **21**, (34), 12629.

28. Wang, W. N.; Ogi, T.; Kaihatsu, Y.; Iskandar, F.; Okuyama, K., *J. Mater. Chem.* 2011, **21**, (14), 5183.

29. Ogi, T.; Iskandar, F.; Nandiyanto, A. B. D.; Wang, W. N.; Okuyama, K., *J. Chem. Eng. Jpn.* 2012, **45**, (12), 995.

30. Lei, W.; Portehault, D.; Dimova, R.; Antoniettit, M., *J. Am. Chem. Soc.* 2011, **133**, (18), 7121.

31. Kaihatsu, Y.; Wang, W.-N.; Iskandar, F.; Okuyama, K., *Mat. Lett.* 2010, **64**, (7), 836.

32. Gatta, G. D.; Rotiroti, N.; Fisch, M.; Armbruster, T., *Phys. Chem. Miner.* 2010, **37**, (4), 227.

33. Garvie, L.; Hubert, H.; Rez, P.; McMillan, P.; Buseck, P., *J. Alloy. Compd.* 1999, **290**, (1), 34.

34. McMurry, J.; Fay, R., Chemistry (ed.). In New Jersey: Prentice Hall: 2001.

35. Tarrio, C.; Schnatterly, S., Phys. Rev. B 1989, **40**, (11), 7852.

36. Wu, Q.; Hu, Z.; Wang, X.; Lu, Y.; Chen, X.; Xu, H.; Chen, Y., *J. Am. Chem. Soc.* 2003, **125**, (34), 10176.

A novel direct white light emitting phosphor material was prepared from rare-earth free precursor solution.